NBSIR 75-804

GENERATION OF STANDARD EM FIELDS FOR CALIBRATION OF POWER DENSITY METERS 20 kHz to 1000 MHz

M.L. Crawford

Electromagnetic Division
Institute for Basic Standards
National Bureau of Standards
Boulder, Co 80302

January 1975

Final Report

U.S. DEPARTMENT OF COMMERCE, Frederick B. Dent, Secretary

NATIONAL BUREAU OF STANDARDS, Richard W. Roberts, Director

CONTENTS

LIST OF FIGURES

GENERATION OF STANDARD EM FIELDS FOR
CALIBRATION OF POWER DENSITY METERS
20 kHz to 1000 MHz

        This report describes techniques for cali-
brating power density meters used by the Department
of Defense in measuring high intensity (hazard level)
RF fields in the frequency range 20 kHz to 1000 MHz.
It reports on part of the work sponsored by the
Calibration Coordination Group (CCG), of the Depart-
ment of Defense covering the frequency range 20 kHz
to 20 GHz.
        Several techniques were considered for pro-
ducing a standard field including parallel plate
and parallel wire transmission lines, transverse
electromagnetic mode (TEM) transmission cells,
various directive antennas and open ended waveguide
(OEG). The major emphasis in this report is on
the TEM cells, which are recommended for the fre-
quency range 20 kHz to 500 MHz. Design and evalua-
tion details and an error analysis associated with
the TEM cell measurement system are given. Power
density levels can be established in the cells from
a few $\mu W/cm^2$ to 100 mW/cm^2 with uncertainties less
than $\pm$ 1 dB.
        Limited information is also given describing the
use of OEG, the recommended technique for the frequency
range 500 MHz to 2.6 GHz, and giving the results of
intercomparisions among parallel plate lines, TEM
cells, OEG, and standard gain horns.

Key words: Hazard level fields; power density meter
calibration; TEM transmission cells.

1.   Introduction

There is increasing concern among military and civilian
agencies about the effects of non-ionizing (RF) radiation on
equipment and personnel. For example, potentially hazardous
electromagnetic (EM) radiation may occur near radar or radio

antennas, or may be produced by electric appliances such as microwave ovens. There are several types of commercial meters now being used to survey the strength of EM radiation. This report describes work performed under the sponsorship of DoD/CCG to develop and evaluate instrumentation and standard techniques for generating known RF fields in order to calibrate these radiation meters.

The objective was to develop optimum procedures for calibrating power density meters used by the DoD for measuring high-intensity (hazard level), free space RF fields over the frequency range 20 kHz to 20 GHz. The required power density levels are approximately 1 to 100 mW/cm^2 or E field strengths of 60 to 600 V/m. The desired calibration accuracy is ± 1 dB. This report describes techniques for use below 1000 MHz, with emphasis on the TEM (Transverse Electromagnetic Mode) cell which is recommended for use over the 20 kHz to 500 MHz range. The companion report will describe in more detail the techniques which are recommended in the frequency range 500 MHz to 20 GHz.

A number of alternative techniques were evaluated and compared for ease, accuracy, and cost of duplicating the measurement procedures. These techniques are described briefly in section 2 of this report and include: (a) producing a uniform field between two parallel plate conductors or between two parallel wire lines, (b) generating a uniform field inside TEM transmission cells or waveguide, (c) producing a calculable field in front of directive antennas such as a standard gain horn or open-ended waveguide (OEG). The advantages and limitations of the various approaches are given to justify the choice of the recommended techniques (i.e., TEM cells and OEG). Sections 3, 4, and 5 describe the TEM cell method in considerable detail, since it is recommended over a large portion of the frequency range (20 kHz - 500 MHz). Details for using OEG over the frequency range (500 MHz - 2.6 GHz)

will be given by Bowman in a companion report and are not
repeated here. However, some of the background leading to
the selection of OEG is included, along with results of some
intercomparisions among parallel plate lines, TEM cells, OEG,
and standard gain horns. These measurements were made at
overlapping frequencies to strengthen the credibility of the
particular approach and provide verification for the accuracy
statements included in the error analysis portion of this
report. These results are contained in section 4 and indi-
cate excellent agreement, well within the prescribed accuracy
limits (± 1 dB) attributable to these particular measurement
techniques.

2. Techniques for Generating Standard Test Fields

2.1 Parallel Plate Transmission Lines

This technique has been in use for some time for EM pulse
studies and for susceptibility testing of electronic equipment.
Various authors have presented the technique in detail [1,2],
hence only a brief description will be given here. Essentially
the test field is established between the conducting planes of
a parallel-strip transmission line (figure 1) which is termi-
nated with its characteristic impedance and driven by a high
power RF source through an impedance matching network. Static
field analysis given in reference [1] shows the TEM mode of
a parallel plate line can simulate a free-space plane electro-
magnetic wave over a substantial portion of its interior
region.

The impedance of the line, neglecting fringing, is
given approximately by

$$Z_o \simeq 377 \, \frac{h}{w} \text{ ohms.} \tag{1}$$

where h and w are as shown in figure 1. The electric field is given as

$$E_v = \frac{V}{h} \text{ volts/meter.} \tag{2}$$

For the line shown, field strengths in excess of 200 V/m can be obtained using 100 watt generators.

This system can be used at frequencies up to a few hundred MHz with a fair degree of accuracy if the test item, or hazard probe, is small (< h/5xw/5). However, as the frequency increases and h approaches $\lambda/4$, the line radiates strongly from the open sides. This creates interference which may interact with the measurement itself, be hazardous to an operator, or interfere with other experiments being conducted within transmission range. Also higher order modes will exist whenever the plate separation exceeds $\lambda/4$. These modes distort the test field configuration and limit the accuracy in determining the known field. The main disadvantages are then the size limitations imposed by the upper useful test frequency and the lack of shielding to prevent radiation. The system must also be carefully impedance matched and the dimensions of the device being tested should not exceed (h/5xw/5). Otherwise large standing waves can exist within the test region and the electric field will be significantly different between the test item and the plates than indicated by field calculations based upon the RF voltage measured between the plates. Construction costs are minimal for building a line capable of testing probes up to approximately 10 cm size, at frequencies up to 100 MHz. Parts plus labor should not exceed $2,000-$3,000.

A parallel plate line was constructed at NBS and used at 15 MHz to calibrate a dipole transfer standard probe for intercomparing with similar calibrations using a TEM transmission cell. The results of this comparison are contained

in section 6. Errors associated with the parallel plate transmission line technique are similar to those described in evaluating the TEM transmission cell and are believed to be within the desired calibration accuracy of ± 1 dB.

2.2 Parallel Wire Transmission Line

This technique is very similar to the parallel plate line except it utilizes electrically balanced wires in place of electrically balanced or unbalanced plates. Since typical power density meter probes are small, the spacing between conductors of a parallel wire transmission line can be kept small thus making this technique appear feasible for generating a standard test field [3]. The field midway between the conductors is approximately uniform if the wire diameter is significantly less than the spacing between conductors and is given by

$$E_v \cong \frac{377}{\pi d} |I_\ell| \tag{3}$$

where I_ℓ is the current in the conductors, and d is the half distance separating the two conductors of the transmission line. The characteristic impedance of open two-wire line in air is given as:

$$Z_o = 120 \cosh^{-1} \frac{2d}{a} \tag{4}$$

where d is a defined above and a is the conductor diameter. The line current I_ℓ is determined by terminating the line in its characteristic impedance (approximately 600 ohms), accurately measuring the resistance R of the termination, the power P dissipated in R, and using the relation

$$|I_\ell| = \sqrt{P/R}. \tag{5}$$

A block diagram of the line and associated equipment is shown in figure 2. The thermopile is used to compare the heating effect of the RF power in the terminating resistor to an equivalent dc power which is measured with the dc voltmeter.

5

This technique suffers from essentially the same dis-
advantages as the parallel plate line with the added dis-
advantage of less field uniformity; thus no effort was made
to further develop it for calibrating power density meters.

2.3   TEM Transmission Cells

This technique utilizes a transverse electromagnetic
(TEM) transmission cell that operates as a 50Ω impedance-
matched system (figure 3). A calculable, uniform TEM field
is established inside the cell at the test frequency of
interest by coupling RF energy through the cell from a trans-
mitter connected at the cell input port. A 50Ω (reflectionless)
termination is connected at the cell's output port. This tech-
nique operates essentially the same as a parallel plate line
except it has the major advantage of not radiating energy
into the surrounding space, i.e., the EM field is contained
inside the cell. It is extremely broadband in frequency,
being limited only by the waveguide multimode frequency asso-
ciated with the cell size. The cells are inexpensive to
construct, approximately $3,000 per cell and the use of ex-
pensive anechoic chambers or shielded enclosures are unneces-
sary. The cells can be used to establish known field strength
levels from below 1 V/meter to 600 V/meter with uncertainties
less than ± 1.0 dB. This technique proved to be the optimum
procedure for establishing standard fields for calibrating
power density meters at frequencies below about 500 MHz.
(Details of this technique are contained in sections 3 through
5.) At frequencies above about 500 MHz, the small physical
size of the cells (required to prevent multimoding) provides
too small a test region for use with typical commercially
available units, and alternative techniques of producing
known fields are required.

2.4 Directive Antennas

At frequencies above a few hundred megahertz, the most
feasible technique for generating an accurately known cw
calibrating field proved to be by radiation from a directive
antenna. The probe is mounted on a positioner and aligned in
front of the source antenna. Measurements are made by ad-
justing the input power to the source antenna until the desired
power density meter reading is obtained. The standard test
field level, P_d, is then calculated from the following equation:

$$\frac{E^2}{377} = P_d = \frac{P_n \cdot G_p \cdot NZC}{4 \pi r^2} \quad (watts/m^2) \qquad (6)$$

where P_n = net power into the source antenna,

G_p = source antenna power gain,

NZC = near-zone correction factor, which is a function
of r,

r = separation distance between the source antenna
and the probe under test, and

E = standard test field in V/m.

Corrections can be made for the multipath within the chamber by
recording the power density meter reading, P_{indic}, as a
function of r while holding the input power of the source
antenna constant. The correction factor ratio, P_d/P_{indic} (dB),
is then computed as a function of r and averaged to give its
corrected value.

Four alternative source antennas were considered: a) cali-
brated single or multifeed backfire antennas, b) a 4-element
dipole array with calculable gain, c) pyramidal standard gain
horns, and d) calibrated "short horns" or open-ended waveguides.

Short backfire antennas, shown in figure 5, were considered
because of their relatively high gain [4], ($\geq$ 15 dB), thus
requiring less source power. Two short backfire antennas
patterned after figure 5 were constructed at NBS to operate

centered at approximately 500 MHz and 1.0 GHz, respectively. Their gain characteristics were determined as a function of frequency variations about their particular design frequency and found to be quite dependent upon the length and spacing of the feed dipole elements. This type of antenna has considerable potential as a gain standard in the VHF-UHF range but will require additional effort to completely characterize it. The required measurement separation distance between the antenna and a hazard meter to be calibrated (based upon a given multiple of a^2/λ where a is the diameter of the back reflector) is large for this antenna, thus nullifying part of the advantage achieved by the higher gain.* At present, the backfire antenna is useful only as a transfer standard because its on-axis gain cannot be calculated directly.

The four element dipole array over a ground plane (figure 6) on the other hand has considerable gain and can also be characterized mathematically [5]. Work is presently underway at NBS to carefully evaluate this antenna between the frequencies 500 MHz to 2000 MHz for potential use in establishing calculable standard fields. This antenna, however, also has a large aperture, its gain is quite frequency dependent, and it is awkward to use because of the weight and size. Both this antenna and the backfire antenna are more suitable for generating fields over larger test areas than are required for hazard probes.

---

*To establish intense EM fields over a small region for calibrating EM hazard meters with a minimum of required oscillator power, the main consideration is the aperture size of the radiator. It is easy to show (and is shown in the companion report by R.R. Bowman) that for the usual antenna designs and for a separation distance of a given multiple of a^2/λ, where a is the larger aperture dimension of the radiator, the field intensity is a maximum for a given input power when the aperture area is minimum.

Well characterized (on axis gain calibration $\leq$ 0.3 dB) pyramidal standard gain horns are commercially available at frequencies above a few hundred megahertz. However, they also have the disadvantage of being large and cumbersome at frequencies below about 2.6 GHz, and lend themselves to generating fields over larger test areas than required by hazard probes. Their size and subsequent large a^2/λ measurement distance required to minimize the near-field correction error make indoor measurements difficult if not impossible. Standard fields were generated at 500, 750, and 1000 MHz using standard gain horns on a large outdoor extrapolation range for comparison with the TEM cells and OEG radiators. Results of these measurements are contained in section 6. For routine hazard probe calibrations, however, at frequencies below 2.6 GHz, use of standard gain horns is not considered practical.

The OEG (figure 7) is significantly smaller than any of the other three types of antennas considered, and was selected as the preferred option for calibrating small probes over the 500 MHz to 2.6 GHz frequency range. There are several reasons for this: (1) the small aperture area means less oscillator power is required; (2) the front-to-back pattern ratio is satisfactory despite the low directivity of OEG; (3) the entire frequency range from 2.6 GHz to below 500 MHz is covered by commercially available rectangular waveguides with precisely scaled dimensions, permitting gain measurements for one frequency band to provide the basis for calibrations throughout this frequency range; (4) along the radiation axis, at least, the backscatter from fields incident on OEG is quite small; (5) while the reflection coefficient of OEG is fairly large, it is small enough (< 2.1 VSWR) to be connected directly to many commercial traveling-wave-tube (TWT) amplifiers or oscillator without causing damage to the oscillator;* (6) the

---

*We recommend using isolators in the circuit to protect the oscillator against possible accidental damage, even though the antenna does have a relatively low VSWR.

9

gain and the near-field corrections for OEG are smooth and almost linear functions of frequency; (7) the relatively small size of the OEG simplifies its mounting, alignment, and handling.

Complete, high-accuracy measurements of the gain of OEG (using WR450), were made for this project. Further, assertions (2), (4), (5), and (6) above, which are not obvious, have been experimentally established. Details of these tests, along with formulas and graphs for the gain and for approximate near-zone corrections for waveguide sizes WR1500, WR975, WR650, and WR450 will be given by Bowman. His report will also present an error analysis and give the measurement procedure for using OEG and standard gain horn radiators to establish standard test fields and hence are not repeated here.

The relatively low directivity of OEG causes a strong illumination of the surrounding test chamber which then produces a relatively large amount of backscatter in the test chamber. However, calculations indicate that this effect will be more than compensated by the fact that the probe under test can be brought much closer to low-directivity radiators than to high-directivity radiators. This was verified by moving the probe along the radiation axis and observing the response perturbations due to multipath interference (MPI). Despite the small dimensions of our test chamber (about 3.5 by 3.5 by 5 meters) and the fact that our radiation absorbing material is less than the best available, the MPI perturbations were less than ± 0.2 dB for all frequencies when using the OEG radiators. These measurements were made for an EM hazard meter that had a response pattern that was essentially isotropic. Therefore, unless a probe is being calibrated that does not have its maximum response pattern directed toward the radiator, these MPI perturbations should represent the maximum that would be observed on any high quality indoor range with equal or larger dimensions than 3.5 m by 3.5 m by 5 m long.

3. Description, Design and Evaluation of the TEM Cells

(Recommended techniques for calibrating power density meters from 20 kHz to 500 MHz.)

The cells (figure 8) consist of a section of "rectangular coaxial" transmission line tapered at each end to adapt to standard coaxial connectors. The line and tapered transitions have a nominal characteristic impedance of 50 ohms (real) along their length to insure minimum voltage standing wave ratios (VSWR). The electromagnetic (EM) field is developed inside the cell when RF energy is coupled to the line from a transmitter connected at the cell input port. A matched 50 ohm termination is connected to the output port. The fields inside the cell were monitored using special electric and magnetic field probes designed and constructed by NBS [6].

Experience with the cells show that at frequencies for which only the principal wave (TEM mode) propagates through the cell, a reasonably uniform electric field can be generated. The major design considerations are to:

1. maximize usable test cross sectional area,
2. maximize upper useful frequency limit,
3. minimize cell impedance mismatch or voltage standing wave ratio,
4. maximize uniformity of EM field inside the cell.

The cells were designed using experimental modeling* and the approximate equation for the characteristic impedance of shielded strip line [7]

$$Z_o \simeq \frac{94.15}{\sqrt{\epsilon_r} \left[\frac{w/b}{1-t/b} + \frac{C'_f}{0.0885\,\epsilon_r} \right]} \quad (\text{OHMS}). \qquad (7)$$

---

*Work is in progress jointly at NBS and the University of Colorado to develop the mathematical formulation to provide a more exact theoretical description of the TEM cell.

In eq. (7), ε_r is the relative dielectric constant of the medium between the conductors, C'_f is the fringing capacitance in pf/cm, and w, b, and t are as shown in figure 9.

The problem of converting the shielded strip line into a "rectangular coaxial" line is primarily one of determining experimentally the value of C'_f. This was done using a time domain reflectometer (TDR) to evaluate a small scale model of the cells. C'_f was found to be approximately equal to 0.053 pf/cm. Dimensions for b were determined from the design criterion that no more than 1/3* of the dimension, b/2, be exceeded by the radiation hazard probe or meter to meet design considerations 1, 3, and 4. Once b and C'_f are determined and an available metal thickness t selected, w can be calculated from (7), assuming approximately 51 ohms, for the line characteristic impedance. (Fifty-one ohms was chosen to allow for some impedance loading effect when inserting the meter inside the cell.) Table 1 gives the dimensions for constructing the cells with specified upper frequency limits. The TDR was then used to make refinements by trimming w until the proper characteristic impedance was obtained.

Table 1. TEM Cell Dimensions

Upper Useful Frequency (MHz)	Plate Separation b cm	w cm	t cm	C'_f pf/cm
100	90	108.15	.157	.053
300	30	36.05	.157	.053
500	18	21.63	.157	.053

*The one third factor is considered a maximum. The impedance loading effect from inserting the meter should not exceed a few ohms if a reasonable VSWR and EM field perturbation is to be maintained.

Figure 10 gives a typical TDR trace of the distributed
impedance along the length of a cell and figure 11 shows
the VSWR as seen at the cell's input and output ports.
The cell distributed impedance as determined by the TDR is
given to a very good approximation by

$$Z_o \simeq \sqrt{L/C} \,. \tag{8}$$

This condition exists since the cell is essentially lossless
at the frequencies of operation.

3.1   Mapping the Fields Inside the Cells

Measurements were made using a calibrated short dipole to
probe the electric field inside the empty cells. The variations
in relative field strength vs. position were determined in the
longitudinal and transverse directions within the cells. The
electric field, E, is essentially vertically polarized in the
region near the center of the cells and gradually becomes hori-
zontally polarized as one moves in the horizontal direction
toward the gap at the side. Both vertical and horizontal
components of E were measured at each point to determine the
total electric field $E = \sqrt{E_V^2 + E_H^2}$ (E_V and E_H are in phase).
The electric field distribution is shown in figure 12. The
electric field in the test regions shown is primarily vertically
polarized ($E_V \gg E_H$). The relative field distribution is
independent of the magnitude of the test field used and the
frequency so long as the frequency is less than the first
order TE mode (TE_{10}) cut-off frequency given approximately
by the following equation in rectangular waveguide [8]

$$(f_c)_{10} \cong \frac{c}{2W}. \tag{9}$$

The equation for determining the cut-off frequency for a
specific higher order mode in general is given approximately

13

by

$$(f_c)_{m,n} \cong \frac{c\sqrt{b^2 m^2 + W^2 n^2}}{2bW}. \tag{10}$$

For eqs. (9) and (10), c = propagation velocity of light within the cell medium in meters/sec. b and W are as shown on figures 8 and 9, and m and n are integers specifying the mode. Due to the symmetry of the empty cell, the TE_{10} mode is not excited. However, as shown in the example of figure 11, the TE_{11} and/or TM_{11} mode can exist contributing to the resonance phenomena displayed by the high VSWR spike. If higher order modes are allowed to propagate, the field con-figuration, which is the vector sum of each contributing mode, no longer has the simple pattern shown in figure 12. Thus higher order modes greatly complicate interpretation of the measured results of the cell and limit the useful upper frequency.

Variations in the electric field strength for the empty cells are less than 0.5 dB for the cross section of figure 9 over the area typically occupied by the meter. Inserting the meter shorts out part of the electric field due to the metal in the sensors and case and increases the indicated field strength in proportion to the percentage cross section occupied. For calibrating small probes or meters (less than 1/5 of b/2) the effect is small and is included as part of the field non-uniformity error treated in section 4. However, for larger probes or meters (> 1/5) this increase in field strength for a constant test input power cannot be neglected and must be taken into account when determining the absolute test field inside the cell.

Leakage around or through the cell's access door is negligible if the door's dimension is kept small compared to the test frequency wavelength and is located in the side wall as high above or below the center septum as possible (where the current flow is a minimum).

14

4. Measurement Procedure

A block diagram of a typical system for making power density meter calibrations using the cell is shown in figure 13. The meter and/or just the probe, is mounted inside the cell centered midway between the top of the cell and the center septum in the desired orientation. The orientation, size, and type (shielded or unshielded, high resistance or metallic, balanced or unbalanced) of interconnecting leads between the hazard meter and its sensor or probe can have a large effect upon the meter's calibration. Tests can be performed with the leads oriented for minimum or maximum field coupling while making the measurements, thus providing data for evaluating the lead contributions to the overall meter calibration accuracy. Minimum lead interaction with the test field is achieved by orienting them in a direction perpendicular to the E field and/or by properly shielding them. Maximum interaction is achieved by aligning them with the polarization of the test field.

The procedure for calibrating the meter from 1 MHz to the multimode frequency is as follows. The generator output is adjusted until the desired hazard meter reading is obtained. The test field is then calculated from the equation,

$$E_v = \frac{\sqrt{P_n R_c}}{d} \tag{11}$$

where P_n is the net power flowing through the cell, R_c is the measured characteristic impedance of the cell at the test location (approximately 51Ω for the example of figure 10), and d is the separation distance between the upper wall and the center plate or septum.

P_n is determined from the power meter readings on the sidearms of the calibrated coupler using the following equation

$$P_n = CR_f \cdot P_{inc} - CR_R \cdot P_{ref} \tag{12}$$

where CR_f and CR_R are the forward and reverse coupling ratios of the bi-directional coupler and P_{inc} and P_{ref} are the indicated incident and reflected coupler sidearm power meter readings. P_n is invariant with position along the length of the cell since the cell is essentially lossless. If R_c is to be obtained from complex impedance measurements made at the cell's input or output port, a Smith chart would be needed to transform the measured impedance plane to the center (location of the item under test) of the cell. From this the real or resistive component, equivalent to R_c can be found. The separation distance, d, can be determined by a simple measurement, in meters, using a centimeter scale or caliper at the point of interest. The calibration factor, CF, for the meter is then given as

$$CF_v = \frac{E_v}{E_{indic}} \quad \text{or} \quad CF_p = \frac{P_d}{P_{indic}} \tag{13}$$

where E_v or P_d is the level of the standard test field (V/m) or power density (mW/cm^2) and E_{indic} or P_{indic} is the indicated meter reading in volts/meter or mW/cm^2. P_d can be calculated from E_v by the equation

$$P_d = E_v^2/3770 \ (\text{mW/cm}^2). \tag{14}$$

Measurements below 1 MHz are made using a voltage monitor tee and RF voltmeter (figure 14) because directional couplers are not readily available at these lower frequencies. Directional couplers and power meters are used above 1 MHz because of the ability to monitor impedance variations in the system when installing the meter inside the cell. When using the system of figure 14, the input voltage to the cell is monitored directly and eq. (11) becomes approximately;

$$E_v \cong \frac{V_c}{d}, \tag{15}$$

16

where V_c is the measured input voltage to the cell and is
approximately equivalent to $V_c = \sqrt{P_n R_c}$ assuming the cell length
is short compared to the test frequency wavelength. The error
analysis then involves evaluating the uncertainty in measuring
V_c as compared to P_n and R_c, and at the frequencies indicated
for these tests, the errors would be about equivalent.

Swept measurements can be made for a fixed orientation
of the meter and/or its probe using the system block diagrams
of figures 13 or 14 assuming the circuit components remain
matched over the desired frequency range and have acceptable
frequency bandwidth characteristics.

An estimated cost for implementing the TEM cell measure-
ment technique is given in Table 2.

Table 2. Measurement System Estimated Cost

	Block Diagram Fig. 13	Block Diagram Fig. 14
TEM Cell	3,500	3,500
100 W RF Generator	10,000	10,000
Low-Pass Filters	1,200	1,200
Signal Sampler	100	100
Frequency Counter	1,600	1,600
Monitor Tee	--	100
Bi-directional Coupler	600	--
RF Voltmeter	--	700
Power Meters	3,000	--
100 W, 50Ω Termination	300	300
	$20,300	$17,500

Much of this equipment is already available in DoD labs thus
reducing the initial capital expense considerably. The system
of figure 14 could be used over the complete frequency range
20 Kc to 500 MHz using appropriate filters, etc., but with
some loss in accuracy at the higher frequencies.

5. Error Analysis for Standardization of the Field Inside the Cells

A brief discussion of the sources of error in establishing the standard test field inside the cell is given below. The total fractional error, $\delta E_v = \dfrac{\Delta E_v}{E_v}$ in determining the absolute field strength, E_v, inside the cell is given as

$$\delta E_v \simeq \frac{1}{2}(|\delta R| + |\delta P|) + |\delta d| + |\delta E| \tag{16}$$

where $\delta P = \dfrac{\Delta P_n}{P_n}$, $\delta R = \dfrac{\Delta R_c}{R_c}$, $\delta d = \dfrac{\Delta d}{d}$, and δE is the error due to the nonuniformity of E_v determined experimentally by mapping the field distribution in the test region of the cell. Equation (14) was derived by substituting $P_n' = |P_n + \Delta P_n|$, $R_c' = |R_c + \Delta R_c|$, and $d' = |d + \Delta d|$ into eq. (11) and adding δE (obtained from E field mapping). Higher order terms contributing to small errors were then dropped in the derivation to arrive at eq. (16).

The error δP is due to uncertainties in the coupler calibration, the absolute measurement of RF power on the sidearms of the coupler, and impedance mismatches between the cell, coupler, RF source, and cell termination. If a precision calibrated coupler and power meter are used and the cell and its termination are impedance matched (VSWR $\leq$ 1.05), δP should be less than ± 5%.

The error, δR in determining R_c is a function of (1) the measurement accuracy of the TDR, and (2) the impedance loading of the meter inside the cell. If the meter occupies a small portion of the cell ($\leq$ 1/5 of any dimension, b/2, w, or L), δR will be small ($\leq$ 3%), and is typically not corrected for in the calculation of E_v. For larger meters (occupying up to 1/3 of b/2, w, or L), however, the impedance loading effect

must be measured and used to correct R_c when using eq. (11) to calculate E_v. δR for these cases can be much larger but typically would be less than 10% if the hazard probe or meter is centered inside the cell. Exceeding the 1/3 load factor is not recommended.

Determining δE is more difficult. Introducing the meter inside the cell perturbs the electric field distribution as described in the section on field mapping. This loading factor (increase in E) is determined using the small calibrated probes referred to earlier. Because of the difficulty in accurately determining the interaction between the meter and the cell,* the probes are used only to determine error limits. If the size of the meter is less than the 1/5th factor δE is less than 6%. Larger meters necessitate measuring the field distribution around the meter and probe and a higher estimate of δ_E is required. The sources of errors are summarized in Table 3.

6. Intercomparison of Parallel Plate Line, TEM Cells, OEG and Standard Gain Horns

An Intercomparison of the standardized test fields developed between a parallel plate transmission line and inside a TEM cell was carried out using a special NBS dipole probe as a transfer standard. The results obtained at 15 MHz using the two techniques are given in Table 4. Agreement between absolute field strengths (generated by the cell and

---

*The presence of the meter in a free space field also perturbs the field but no correction is made since the relationship between its indicated response and the standardized level of the field without the meter present is what is desired. The boundary conditions of the cell, however, modify this relationship and result in an increased E field over what would otherwise be computed from eq. (11). Additional work is required to better establish this relationship.

Table 3. Summary of Measurement Errors

Source of Error	Percent Uncertainty
a. Absolute measurement of incident RF power on the side arm of coupler.	± 3.0
b. Coupler calibration.	± 2.0
δP, total error in determination of RF power passing thru cell.	± 5.0
c. Cell impedance, δR.	± 3.0
d. Cell plate separation, δd	± 1.0
e. Non-uniformity of electric field inside cell, δE.	± 6.0
Maximum Field Strength Error	±11.0
	<± 1.0 dB

$$\delta E_v \simeq \frac{1}{2}(|3| + |5|) + |1| + |6|$$

the parallel plate line) required to produce the same probe output voltage is well within the uncertainties attributed to the different techniques.

Table 4. Intercomparison of NBS TEM Cells* with Parallel Plate Line at 15 MHz Using 10 cm Dipole Probe

Probe Output Voltage	NBS 0.6 m x 1.0 m Cell E_V (V/m)	Parallel Plate Line E_V (V/m)
0.1	21.3	27.0
0.2	34.5	32.0
0.3	47.2	47.0
0.5	71.0	71.5
1.0	127.0	131

Intercomparisons were also made with a calibrated probe to determine agreement in the test field between cells of different sizes and shapes. Table 5 gives the results of these measurements.

Table 5. Intercomparison of Field Strength in Different Sizes and Shapes of TEM Cells as a Function of Frequency* (2 cm reference probe output level set at 100 mv)

Freq. MHz	0.6 m x 1.0 m Cell E_V (V/m)	0.5 m x 0.5 m Cell E_V (V/m)	0.3 m x 0.5 m Cell E_V (V/m)	0.2 m x 0.3 m Cell E_V (V/m)
65	26.1	24.5	25.6	--
100	24.1	24.5	24.8	--
150	23.0	22.5	23.8	--
200	24.6	22.2	24.5	22.0
250	20.3	23.2	22.6	--
300	--	24.4	23.5	--
400	--	--	21.5	22.4
500	--	--	20.0	22.0
600	--	--	--	23.2
700	--	--	--	17.5

*Cell dimensions are given in terms of b x W of figure 9.

Finally, intercomparisons of field strength were made using TEM transmission cells, open ended waveguide radiators, and standard gain horn radiators to establish standard test fields in the frequency range 500 MHz to 1000 MHz. Figure 15 is a photograph of the polyfoam tower used to support the hazard probe in front of a standard gain horn on the NBS outdoor extrapolation range. Results obtained by calibrating a 2 cm dipole transfer standard are summarized in Table 6. These measurements indicate that the TEM cell method should be replaced by the OEG or standard gain horn technique above approximately 500 MHz. In general, we recommend use of OEG between 500 MHz and 2.6 GHz because less transmitter power is required (for reasons alluded to earlier in this report and explained by Bowman [1]). Agreement between the three techniques is well within the combined error limits assigned to the particular measurement methods.

Table 6. Intercomparison of Output Voltage From 2 cm Dipole Probe Vs. Frequency Using TEM Cells, Open End Waveguide, and Standard Gain Horns (Standardized Test Field = 1 mw/cm^2).

| | Output of Probe, Volts | | |
Freq MHz	0.2 m x 0.3 m TEM Cell	Open End Waveguide	15 dB Standard Gain Horn
500	.368	.342	.350
600	.353	--	--
750	*.340	.330	.362
1000	--	.373	.400

*Corrected 2.1 dB for multimode propagation effect.

7. Summary and Conclusions

The objective of the work described in this report was
to develop optimum techniques for calibrating power density
meters used by the DoD for measuring high intensity (hazard
level) RF fields, particularly in the frequency range 20 kHz
and 1000 MHz. A number of alternatives for producing stand-
ard EM fields were evaluated from which TEM cells and OEG were
selected. Considered were initial cost, compatibility of cali-
bration system with instrumentation, minimum danger to personnel,
ease of calibration procedures, etc. The TEM cells are ex-
tremely broadband (dc to 500 MHz) and are self-shielding
which eliminates hazards to personnel or equipment and inter-
ference to the same. They are inexpensive to build and have
potential for application for other forms of testing such as
evaluating electronic equipment susceptibility and radiated
emissions, and EM pulsed calibrations. Details sufficient
for construction of the cells are included in the report
along with procedures for implementing them into the calibra-
tion system.

In conclusion, a few comments are in order concerning
extended use of the TEM cells.

1)   Probes or meters of any size could be tested using
a TEM cell modeled from Table 1 and figure 8 to meet the
criteria that the size of the test object should be pre-
ferably less than L/5 x w/5 x b/10. Thus small objects
could be tested at higher frequencies in small cells, and
large objects could be tested at lower frequencies in
large cells. The procedure for testing large objects
is the same as for testing in small cells but a higher
power signal source and termination (50Ω) would be
needed.

2) The upper useful frequency for the cell is reduced
20 to 30 percent from the cutoff/multimode frequency
given in Table 1 to allow for loading effects of the
meter inserted in the cell and to provide sufficient
higher order mode suppression or attenuation.

References

[1] Musil, V.P., Generating high-intensity electromagnetic fields for radiated-susceptibility test, IEEE EMC Symposium Record, Seattle, Wash., pp. 185-194 (July 1968).

[2] Roseberry, B.E., and Schulz, R.B., A parallel-strip line for testing RF susceptibility, IEEE Transactions on EMC, Vol. EMC-7, pp. 142-150 (June 1965).

[3] Lawton, R.A., New standard of electric field strength, IEEE Transactions on Inst. & Meas., Vol. IM-19, No. 1, pp. 46-51 (Feb. 1970).

[4] Ehrenspeck, H.W., The short-backfire antenna, Proc. of IEEE, Vol. 53, No. 8, pp. 1138-1140 (Aug. 1964).

[5] Cottony, H.V., Methods for accurate measurement of antenna gain, NBS Report (unpublished).

[6] Greene, F.M., Design and calibration of E and H field probes for HF band application, Proc. DoD Electromagnetic Research Workshop, Washington, D.C., pp. 50-76 (Jan. 1971).

[7] Skaggs, G.A., High frequency exposure chamber for radiobiological research, NRL Memorandum Report 2218 (Feb. 1971).

[8] Ramo, S., and Whinnery, J.R., Fields and Waves in Modern Radio, p. 367 (Second Edition, Fifth Printing, Nov. 1960).

TOP VIEW

COPPER GROUNDING STRIP

2' MIN

132"

2" X 4" WOOD

THERMO SETTING PLASTIC
LINEN BASE 2 3/8 X 4 X 18 INS

SIDE VIEW

LOAD END

120"

12"

17"

16"

18"

1/8"ALUMINUM SHEET

1/16"ALUMINUM WITH PLYWOOD BACKING

END PLATES ARE MADE FROM 1/32"COPPER PLATE

TYPE N CONNECTOR

INPUT END

SEE ENLARGED DETAIL

24"

23"

10 5"

10"

2"

12

ENLARGED
DETAIL

11"

2"
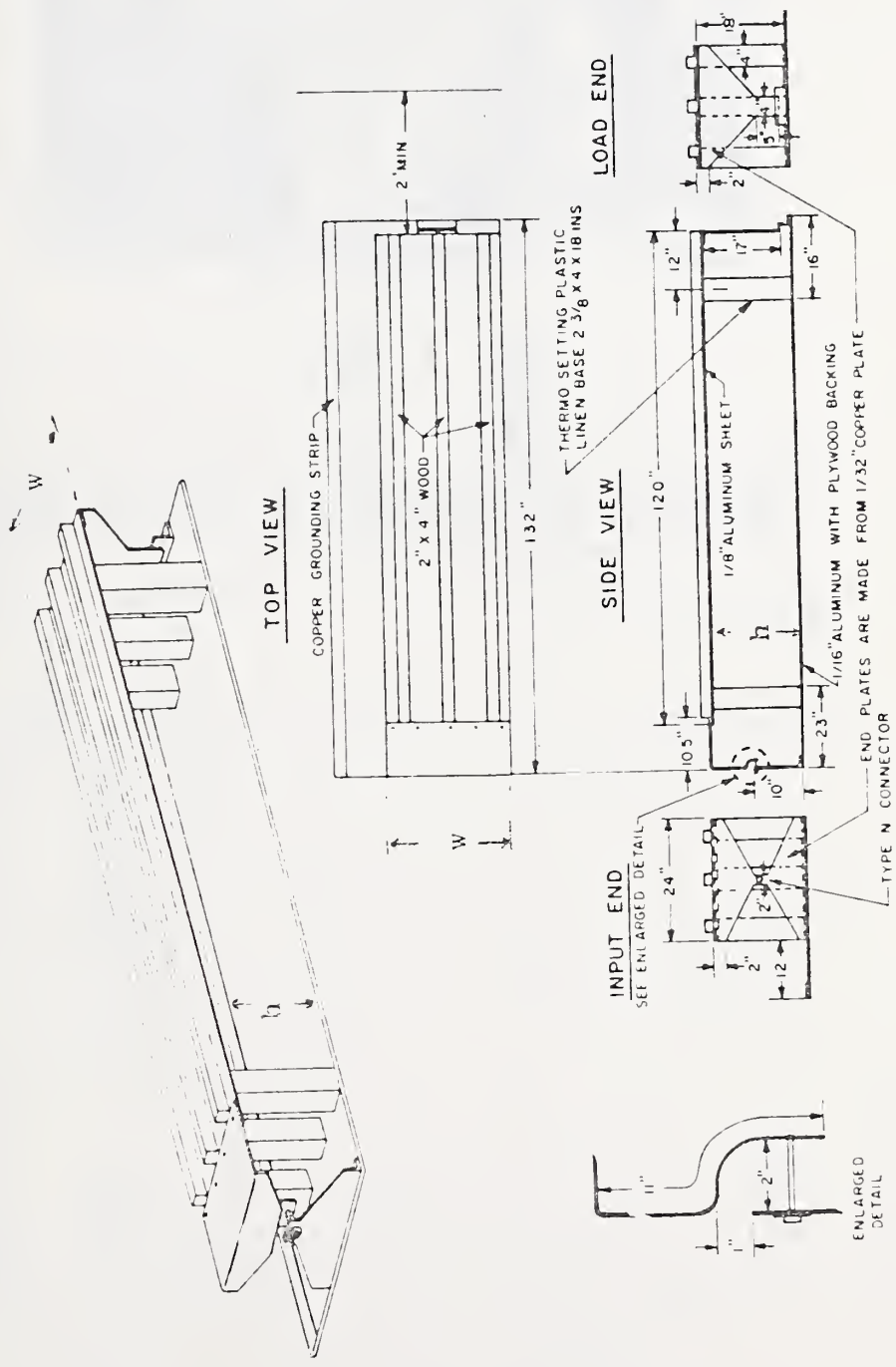
FIGURE 1. TYPICAL PARALLEL PLATE LINE per MIL-STD-462.
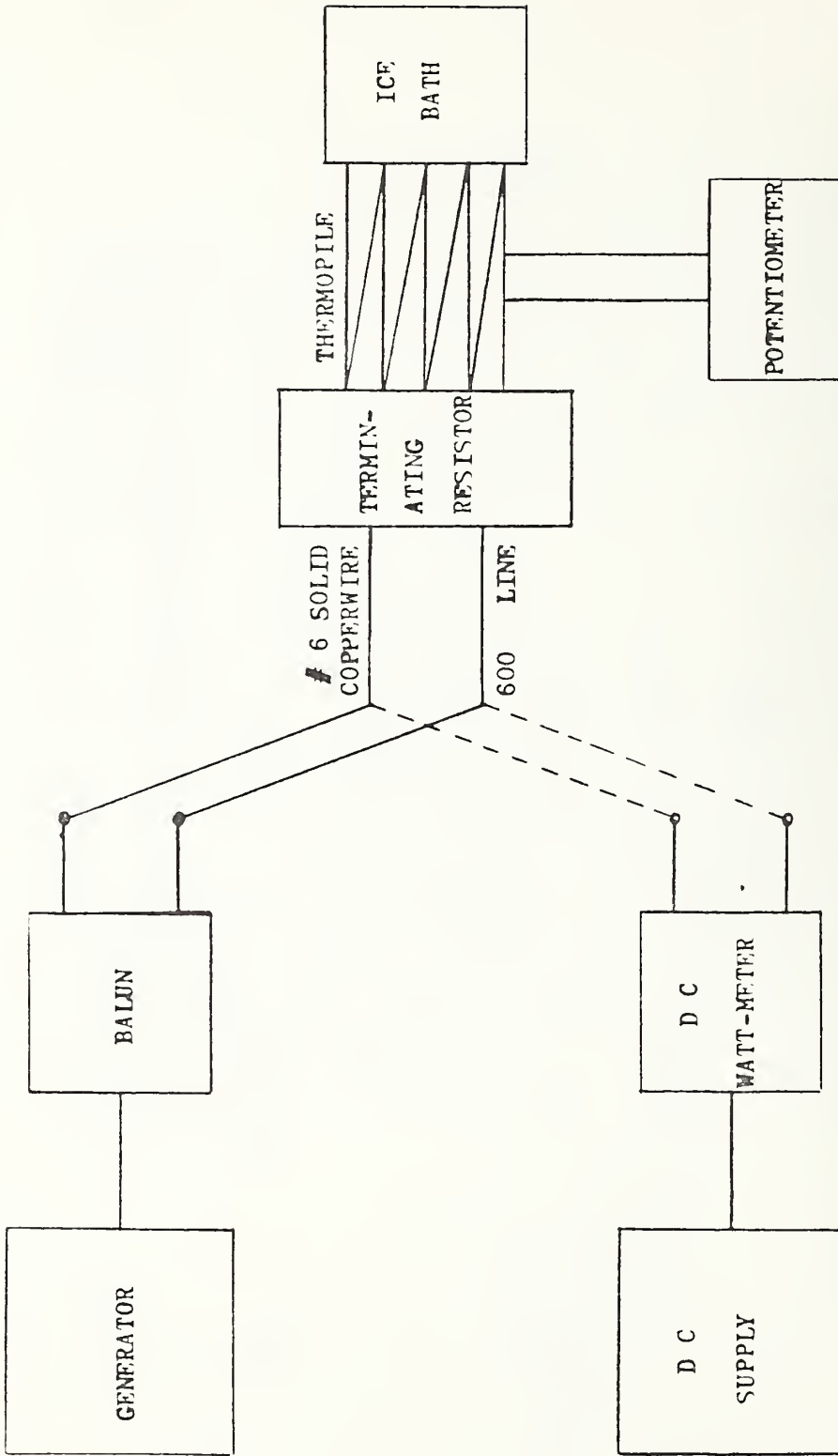
FIGURE 2. BLOCK DIAGRAM OF PARALLEL-WIRE FIELD APPARATUS.
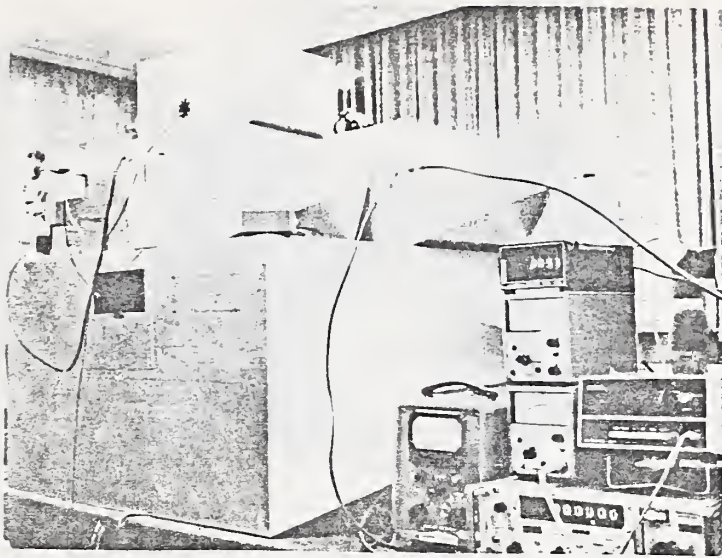
FIGURE 3. TEM CELLS AND ASSOCIATED EQUIPMENT
FOR CALIBRATION OF RADIATION HAZARD METERS.
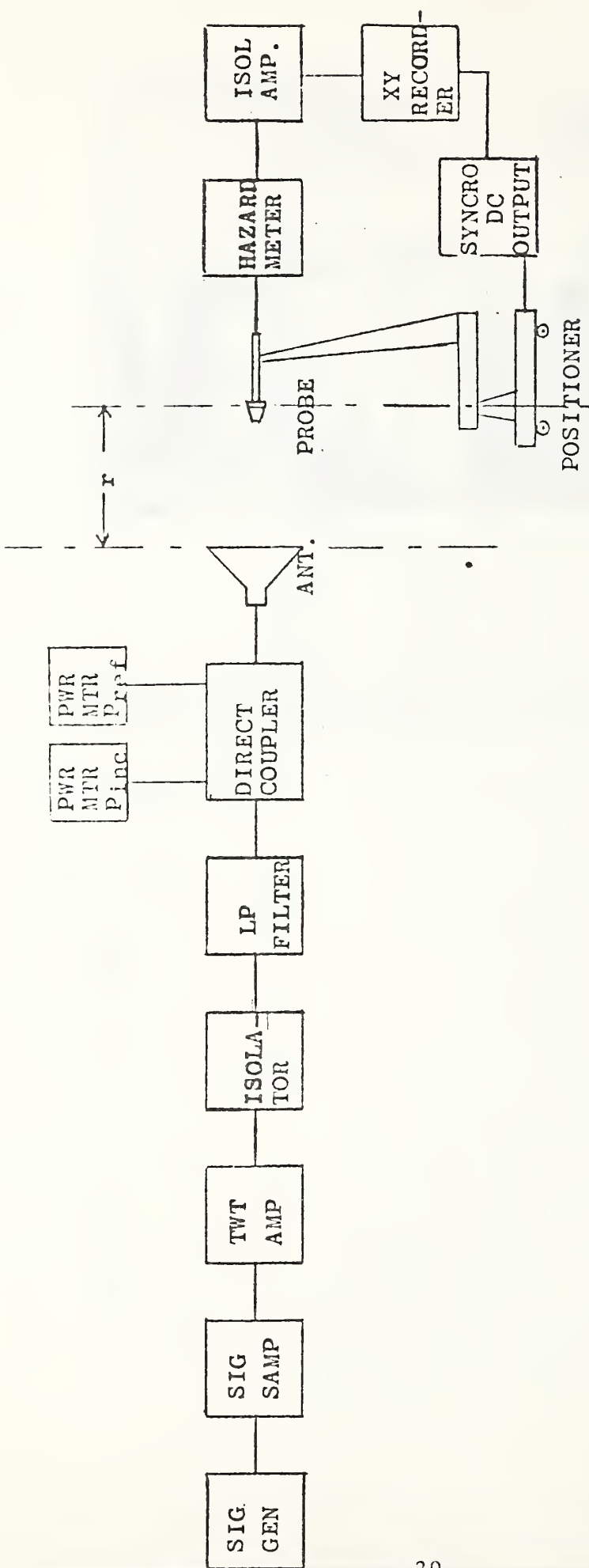
FIGURE 4. BLOCK DIAGRAM OF SYSTEM FOR TESTING RADATION HAZARDS METERS USING DIRECTIVE ANTENNAS.
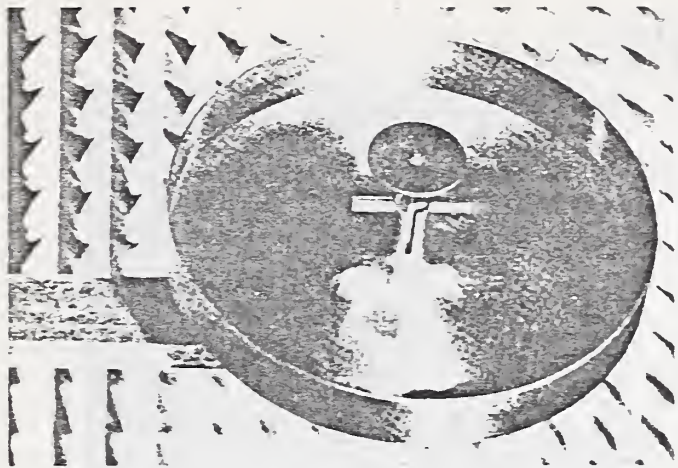
(a)
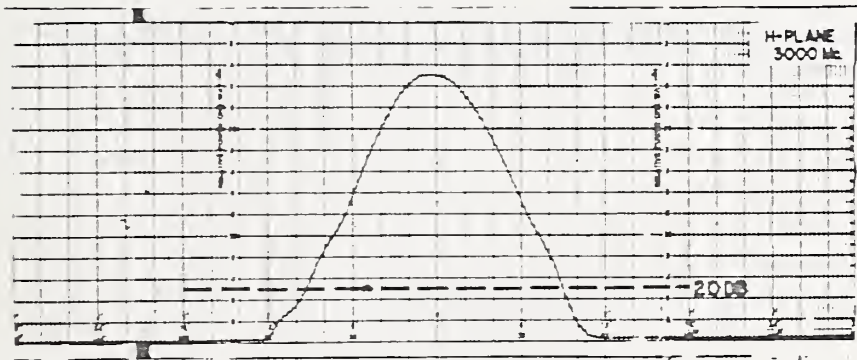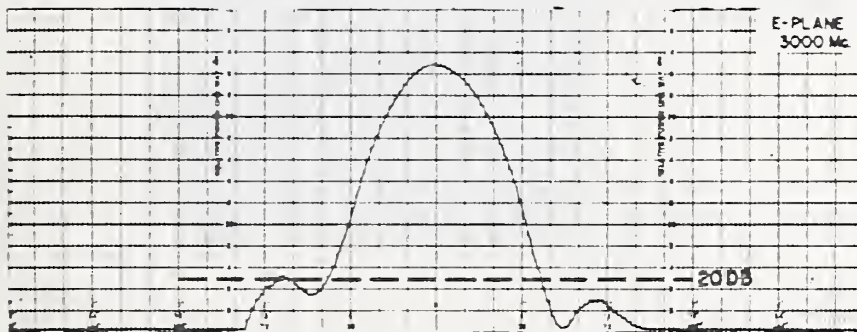
(b)

FIGURE 5. SHORT BACKFIRE ANTENNA WITH RADIATION
PATTERNS.

30
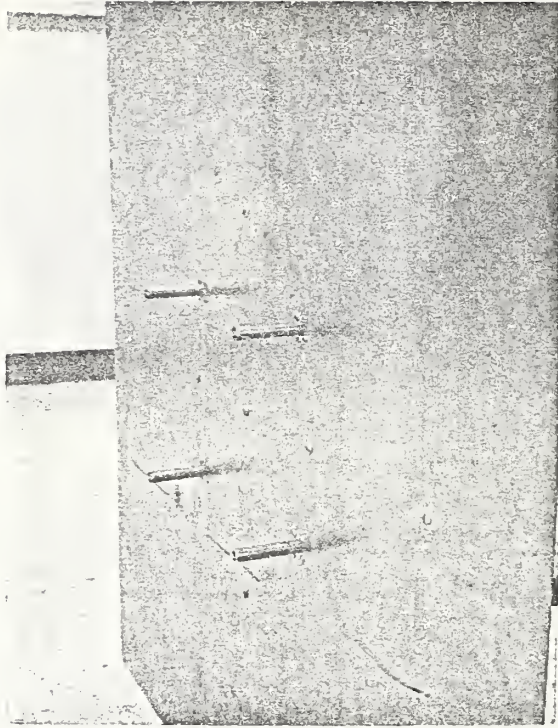
FIGURE 6. FOUR ELEMENT DIPOLE ARRAY ANTENNA.

31
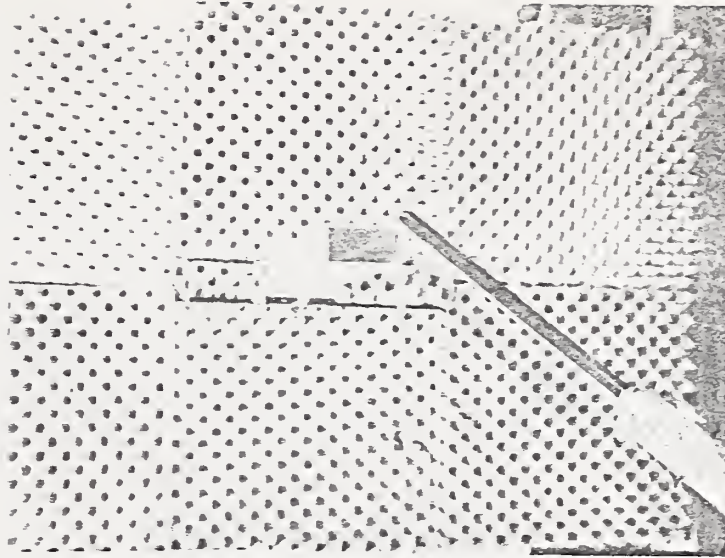
FIGURE 7. RADIATION HAZARD PROBE MOUNTED IN FRONT OF
OPEN-ENDED WAVEGUIDE (OEG) ANTENNA.
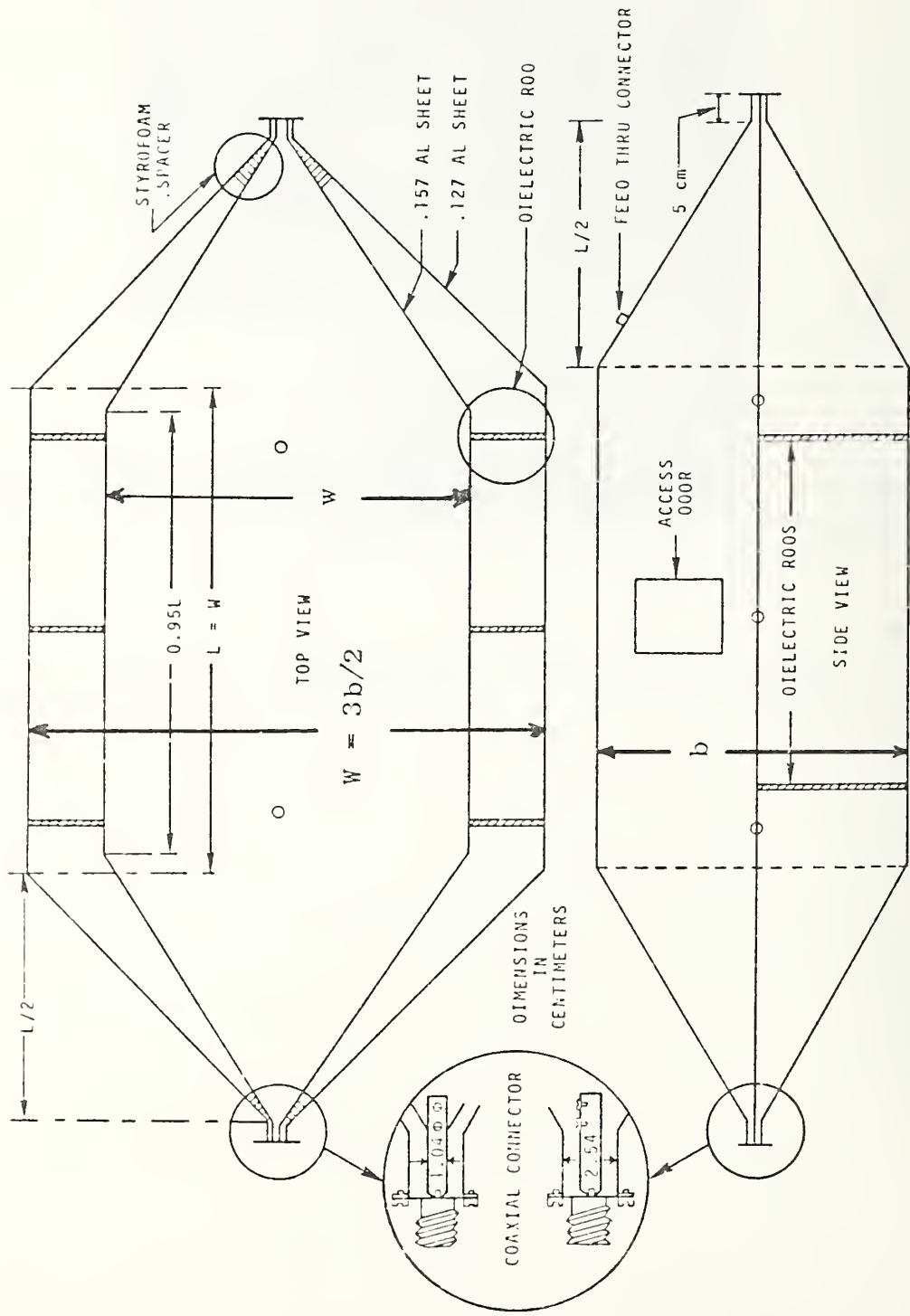
FIG. 8. DESIGN FOR RECTANGULAR TEM TRANSMISSION CELL.
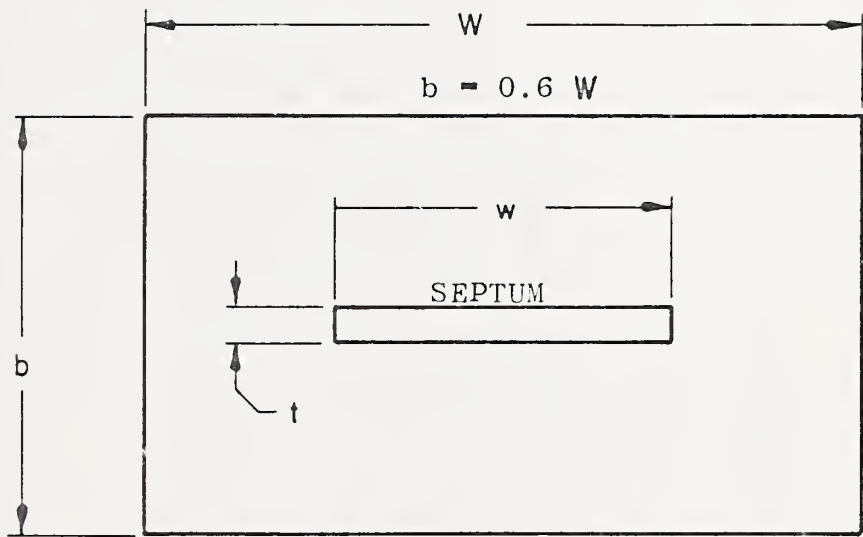
FIGURE 9. Cross Sectional View of Rectangular Transmission Line
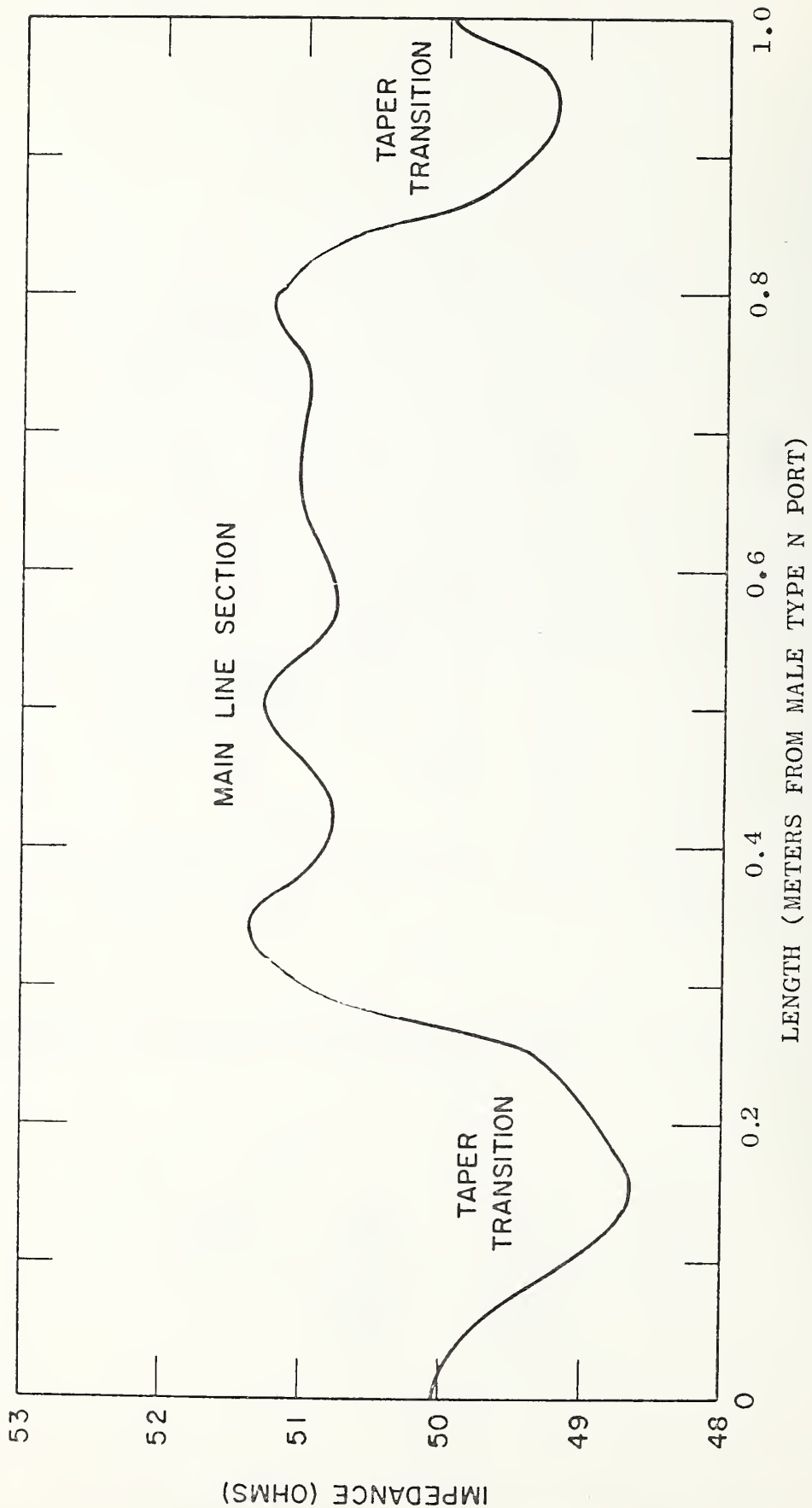
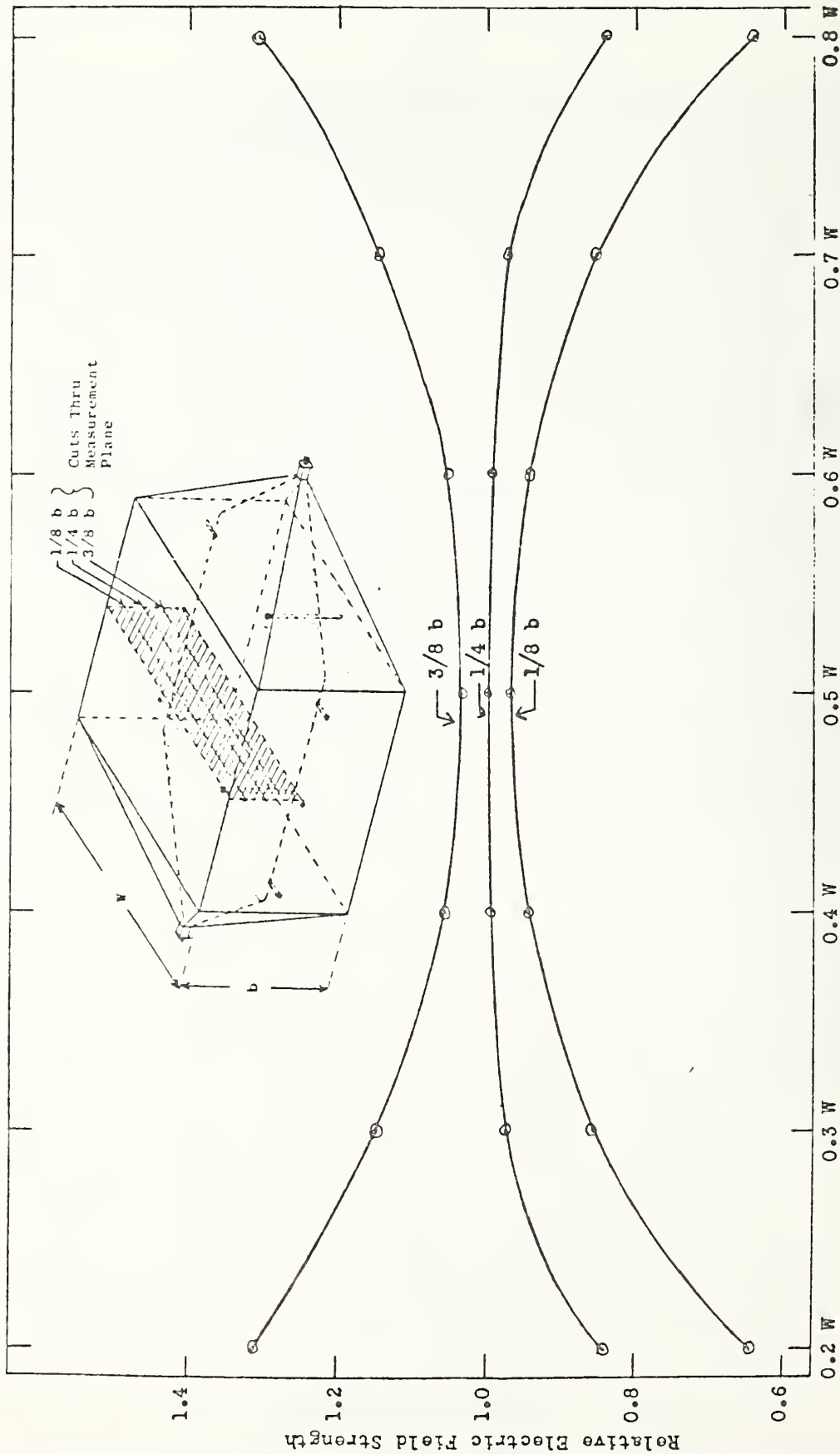Time Domain Reflectometer Trace of Distributed Impedance
of Empty Cell

FIGURE 10.

FIGURE 11.   PORT INPUT
VSWR OF EMPTY CELL.

b x w = 25cm x 42cm
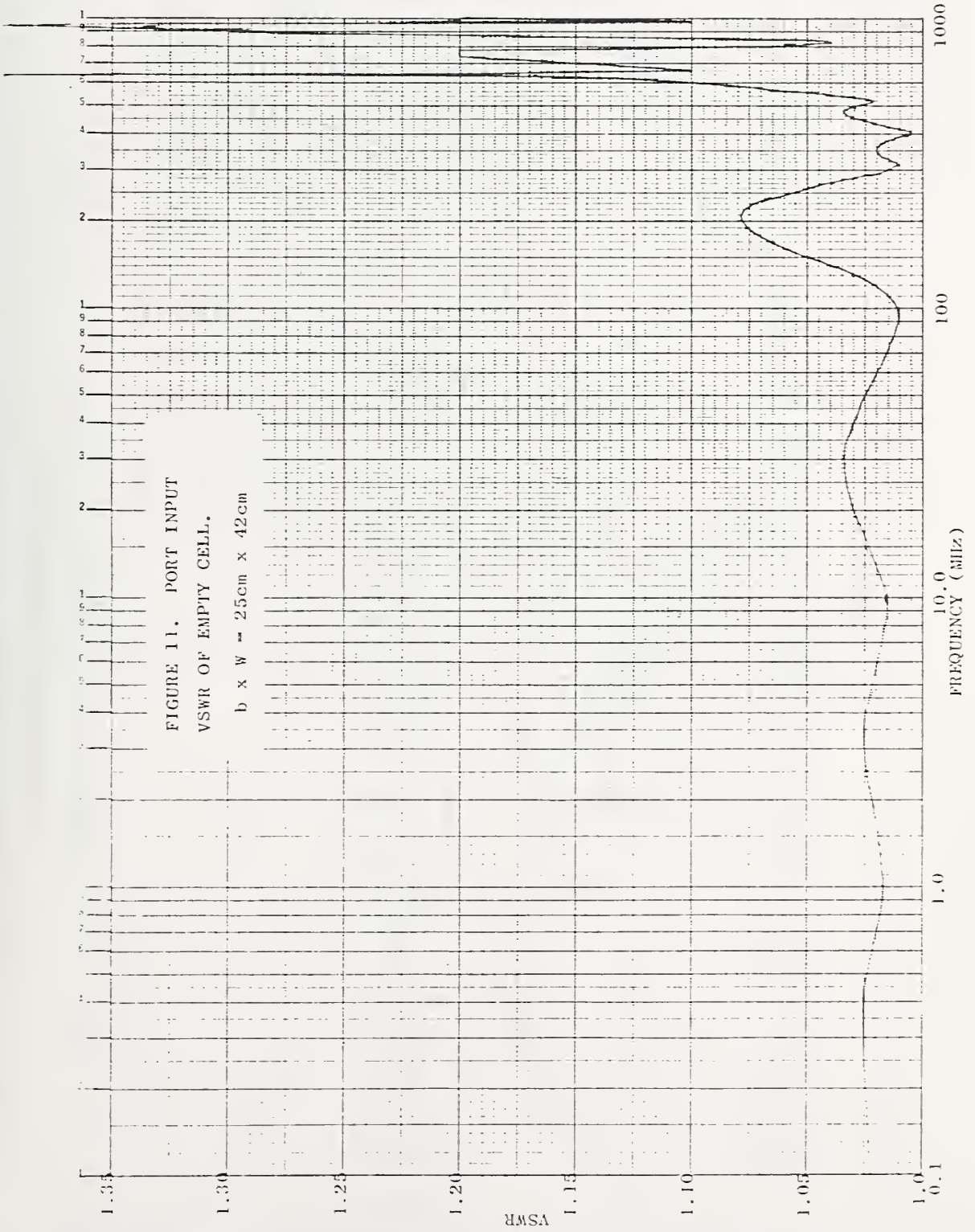
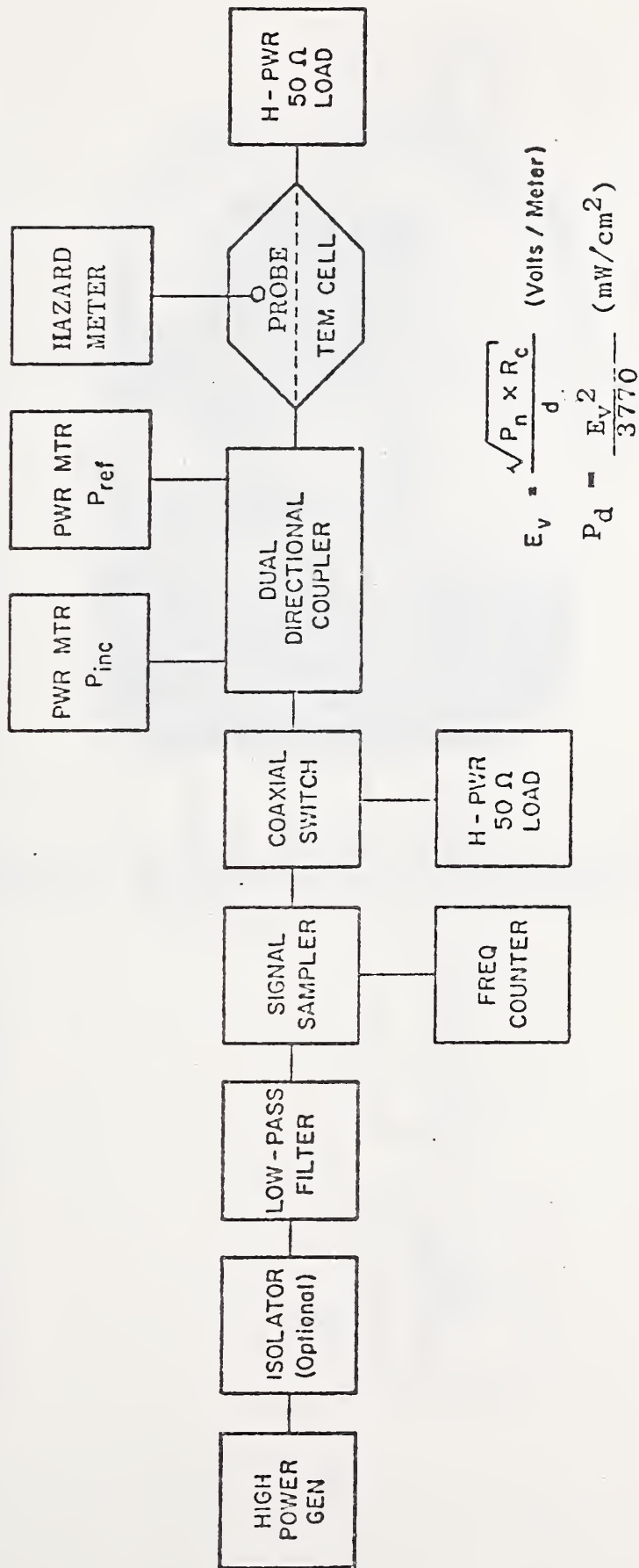FIGURE 12. RELATIVE ELECTRIC FIELD DISTRIBUTION INSIDE CELL. CROSS SECTIONAL CUT THRU UPPER HALF AT CENTER OF CELL.

$$E_v = \sqrt{\frac{P_n \times R_c}{d}} \quad \text{(Volts / Meter)}$$

$$P_d = \frac{E_v^2}{3770} \quad \text{(mW/cm}^2\text{)}$$

FIGURE 13. BLOCK DIAGRAM OF TEM CELL MEASUREMENT SYSTEM FOR RF POWER DENSITY METER TESTING AND CALIBRATION (1 MHz to 500 MHz).
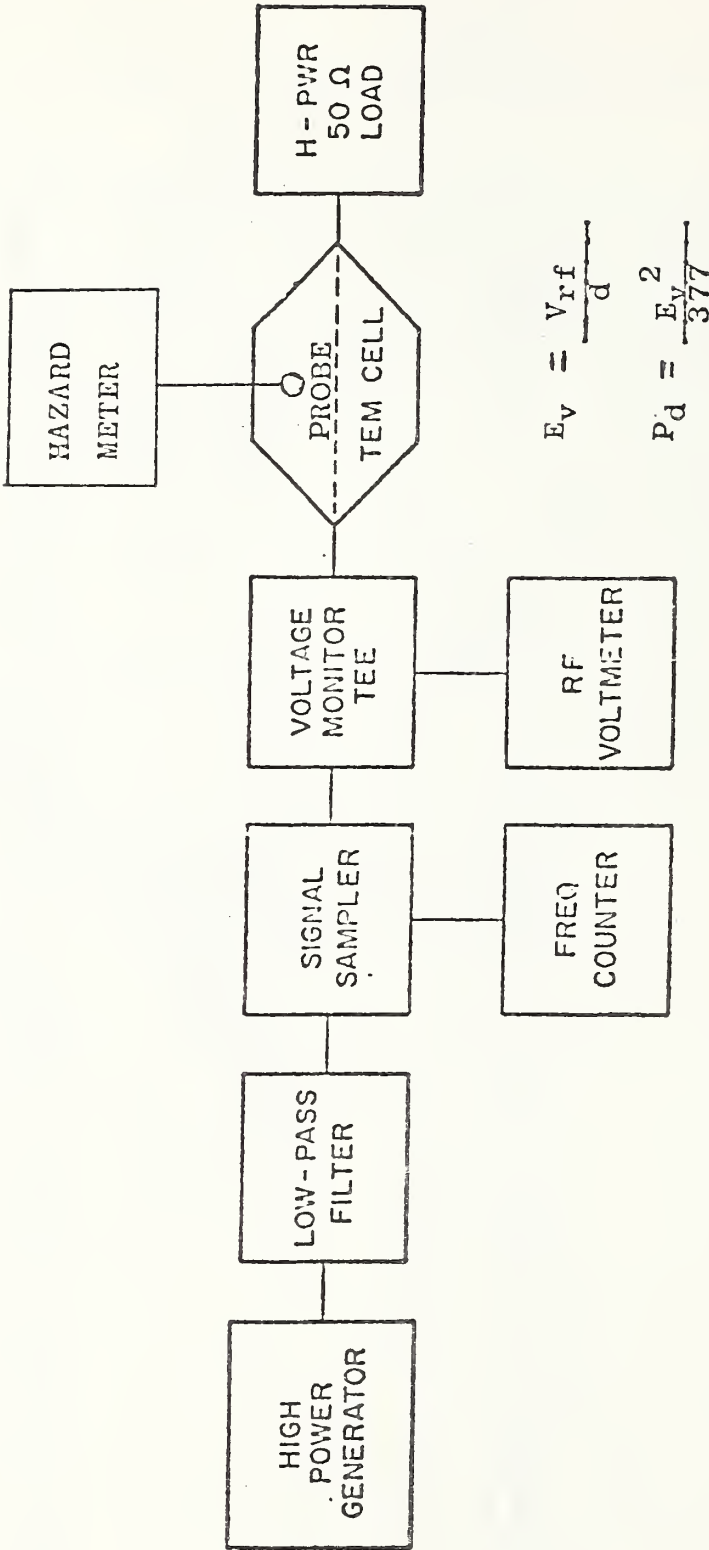
38

FIGURE 14. BLOCK DIAGRAM OF TEM CELL MEASUREMENT SYSTEM FOR RF POWER DENSITY METER TESTING AND CALIBRATION (20 kHz to 1MHz).

$$E_v = \frac{V_{rf}}{d}$$
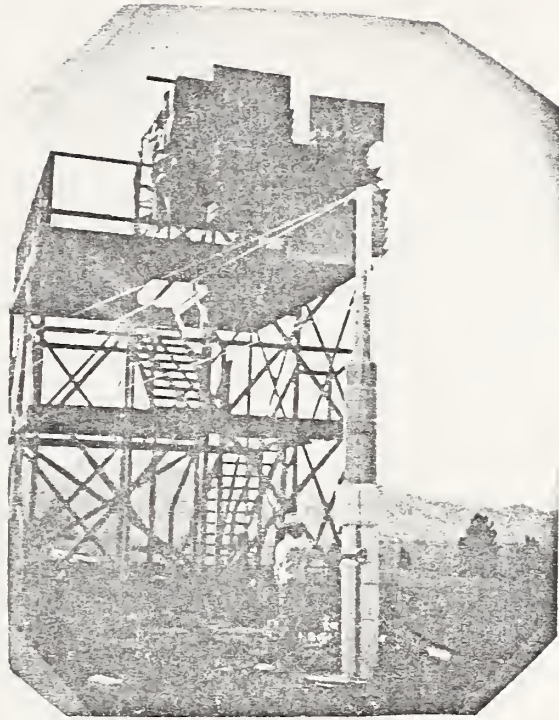
$$P_d = \frac{E_v^2}{377}$$

FIGURE 15.   POLYFOAM TOWER SUPPORTING PROBE IN FRONT
OF STANDARD GAIN HORN ON NBS EXTRAPOLATION RANGE.